В.40
1997

Budker Institute of Nuclear Physics
SB RAS

A. Beklemishev, V. Davydenko,
A. Ivanov, and A. Podyminogin

ASSESSMENT OF THERMO-MECHANICAL STRESSES AND STABILITY OF ION-SOURCE GRIDS WITH PERIPHERAL COOLING

Budker INP 97-75

БИБЛИОТЕКА
Института ядерной
физики СО АН СССР
ИНВ. № 2-й экз

Novosibirsk

Assessment of thermo-mechanical stresses and stability of ion-source grids with peripheral cooling

A. Beklemishev, V. Davydenko, A. Ivanov, and A. Podyminogin

Budker Institute of Nuclear Physics,
630090 Novosibirsk, Russia

Abstract

Application of peripheral cooling for ion-optics grids of diagnostic neutral beam injector is considered. The injector is designed to operate with up to 10 s pulse duration and 1 pulse/5 min repetition rate. The grid deformations under thermoloads during beam-on phase were determined using appropriate semi-analitical model. Distribution of thermo-mechanical stresses over grids and thermo-stability limit as a function of the grids characteristics and heat loads were determinened as well. The simulation results are compared with those obtained in the experiment with the grid prototype.

©Budker Institute of Nuclear Physics,
630090 Novosibirsk, Russia

1 Introduction

It is well known that formation of long pulse ion beams with energy exceeding a few tens of keVs leads to significant heat load on accelerator electrodes due to intense bombardment by ions, secondary electrons and charge-exchange neutrals. Therefore, even if the current density is quite moderate, of the order of 100 mA/cm^2, whenever a beam duration exceeds a few seconds, the temperature rise of the electrodes becomes substantial, requiring their intensive cooling. For this reason, multi-aperture ion-optics systems of powerful injectors are fitted out with the water cooling channels located around the apertures. Due to the required high precision of the beamlets geometry and their relative alignment, fabrication of the inner channels for coolant appears to be quite difficult and expensive. At the same time, quite often, the averaged loads are moderate (tens of watts) compared with those during beam-on phase because of the long intervals between the pulses. If this is the case, rather less expensive and simpler method of edge grid cooling might become applicable. Additional advantage of the grid cooling from periphery is that the grid transparency can be then increased thus leading to higher beam luminosity. We used this approach in order to develop the grids for diagnostic neutral beam injector which will be applied to spectroscopic diagnostics of impurities in the plasma core of the tokamak TEXTOR-94 [1]. Key parameters of the source are: the neutral hydrogen beam current of 1 eq.A incident on the plasma, and the beam energy of 50 keV. Taking the ion species fractions of 90:5:5 % ($H^+ : H_2^+ : H_3^+$) and neutralization efficiency of $\approx$ 50%

into account, an output ion current of 2 A is minimally required in the ion source. An angular divergence of the beam is specified to be less than 1^0. The ion source has to operate in long pulse mode. It has been determined that such a source should provide ten seconds long beam pulses, which is consistent with the time of plasma maintenance in TEXTOR- 94. Each individual pulse consists of a chain of millisecond pulses with millisecond pauses between them, so that total duration of the beam-on time amounts to 5 s.

In the injector ion source the emitter plasma is produced by an inductively excited RF-discharge with a frequency of 5-6 Mhz in a non-homogeneous magnetic field with a maximum of 60G [2]. The beam is to be extracted and accelerated by a four-electrode ion-optics system with slightly concave grids providing beam focusing in TEXTOR plasma at 4 m distance downstream from the ion source.

Under optimal conditions, when most of the particles avoid striking the electrodes, heat loads on those are sufficiently small. Taking this into account, an ion-optics system was developed with grids made of molybdenum plates of sufficiently large thickness and consequently of large heat capacity. Therefore, even without any cooling, their estimated temperature rise during the injector operation remains acceptable. To remove heat from the electrodes between pulses, as well as (partially) during the injection pulse, the electrodes are mounted on water cooled flanges. The suggested grid design seems advantageous from technological viewpoint and enables utilization of the high electric strength of molybdenum. Besides, significantly lower cost of the suggested grid design looks rather attractive for other applications, such as the ion-optics system of long pulse technological ion sources, in which the averaged heat load is moderate due to the small duty factor. Negative consequence of peripheral grids cooling is that under certain conditions the central part of the electrode may be overheated so that significant radial temperature gradients will develop. Corresponding thermal stresses result in radial and longitudinal displacements of electrodes and changes of gaps. To find operational limits of the source it is important to know the displacements which allow for accurate beam formation by the ion-optics system as functions of the thermal loads. The most critical issue here is whether the thermal gradients exceed critical values, above which a sharp instability can develop, leading to drastic variations of electrode bending and large inadmissible changes of gaps between electrodes. Taking this into account, the thermoelastic stresses in the grids should be subjected to serious study. In the present paper we discuss results of calculations of the grid deformations during the beam-on phase and the thermo-mechanical stability of the grids. The paper is organized as follows. In Sec.2 the heat loads on the grids are

specified. In order to estimate the stresses in the grids we have used an idealized analytical model described in this Section. Here is also presented the distribution of the stresses and the corresponding deformations of the grids. Thermo-mechanical stability of the grids with peripheral cooling is discussed in Sec.3. Sec.4 summarizes the main results of the work.

2 Assessment of thermo-mechanical stresses and deformations of the electrodes

In the case of optimal beam formation most of the accelerated ions avoid the electrodes and the main load to electrodes is carried by the secondary particles. Significant fraction of the beam particles can only reach the electrodes in the transitional, quite non-optimal operation modes which take place at the initial application of voltage to the electrodes or after the operation start after break-down. Generally the total duration of such modes (for a few-seconds beams) is not large (less than 1 ms) and the heating by initial particles is not essential. The numerical analysis of the secondary particle trajectories for typical four electrode system was performed in paper [3]. It was shown that the fraction of beam power deposited to electrode is directly proportional to the hydrogen pressure on the beamlet exit and is equal to $\sim 0.8\%$ of the ion beam power, if the pressure in the electrode gaps is in the range of $\sim 3 - 5 \times 10^{-3}$ Torr. The calculated pressure of hydrogen for the planned plasma emitter is close to the given value and thus, the beam power fraction deposited on electrodes can be estimated as 0.8% . The power density at the electrode can be then estimated as $8 \times 10^{-3} \eta j U \approx 24 W/cm^2$. Taking into account the beam duty factor of 0.5, the average power density at the electrodes is $\sim 12 W/cm^2$.

In contrast to other electrodes, the plasma electrode is heated mainly by the primary plasma. If one assumes that each ion-electron pair deposits an energy of 10 eV, at the selected current density of 0.12 A/cm^2 the power density released at the surface will be $\sim 1.2 W/cm^2$. This value is much less than the power density at the surface of extracting and accelerating grids. Of course, we do not take into account the heat loads carried to the electrode by radiation from the discharge, energetic neutrals, etc., which could be significant. Nevertheless, we assume for estimates of thermo-stability limit and deformation of the plates that the maximum heat load is $12 W/cm^2$, as it was estimated for extracting and accelerating electrodes.

Thermal loads to the electrodes may cause significant mechanical stresses

and deformations. In this case, angular spread of the beam will be increased with accompanied increase of the thermal loads on the eletrodes. This makes it necessary to perform numerical calculation of the deformations to select optimal design solutions. In the calculations of the heating and mechanical loads we have used simplified model of the electrodes that in many respects is sufficient to reveal the most critical points of the design. It was taken that in the region occupied by the beam output holes the electrode thickness is the same as in the periphery, but its local heat counductivity χ^*, specific heat capacity C, and the Young modulus E are effectively 2 times less than those on the periphery. This assumption is justified by a 59% transparency of the electrodes. The electrode thickness was initially selected to be 2 mm, the electrode material to be the vacuum melted molibdenum. It was assumed that the thermal load is homogeneously distributed in the region of the holes location on the electrode. The characteristics of molibdenum which were used in the calculations together with the electrode dimensions are given in Table 1.

Table 1: Characteristics of the electrode

Parameter	Value
Electrode radius, a	5 cm
Beam radius, b	3.25 cm
Thermal load on the electrode within r$\leq b$	12 W/cm^2
Thermal lengthening, α	5.1×10^{-6} $^oC^{-1}$ (500^oC)
Thermal conductivity, χ	1.3 $W/(\text{cm } ^oC)$ (500^oC)
Specific heat capacity, C	3.18 $J/(\text{cm}^3\ ^oC)$ (475^oC)
Poisson coefficient, μ	0.324
Young modulus, E	3.3$\times 10^6$ kG/cm^2 (20^oC)
Averaged power on electrode, P	400W

2.1 Temperature profile

The radial distribution of electrode temperature was found from the solution of the thermal conductivity equation:

$$Chf(r)\frac{\partial T}{\partial t} = \chi\frac{1}{r}\frac{\partial}{\partial r}(hf(r)r\frac{\partial T}{\partial r}) + q(r) \qquad (1)$$

together with the boundary conditions

$$\frac{\partial T(t, r=0)}{\partial r} = 0$$

$$-h\chi\frac{\partial T(t, r=a)}{\partial r} = \frac{\chi^* h^*(T - T_h)}{L},$$

where χ^*, h^* and L - are the heat counductivity, thickness and length of the electrode holder respectively, $T_h = 300^oK$ is the temperature of the cooled part of the holder, h=2mm is the plate thickness, f=1 at r$\leq$ 3.25 cm and f=2 at 3.25 cm$\leq$r$\leq$5 cm.

In this case, it was assumed that there was enough time for the temperature to be equalized over the electrode thickness. Equation (1) was integrated numerically using the real differential scheme. In the calculations of heating and tensions which appear during the heating we took the initial temperature of the electrode to be 300^oK. According to the calculation results, the heat sink through the holders appeared to be negligeble compared to the power deposited on the grid. The maximum temperature rise of the electrode was found to be 230^oK at 400 W of total deposited power. The calculated radial profile of temperature on the 10th second of heating is given in Fig.1.

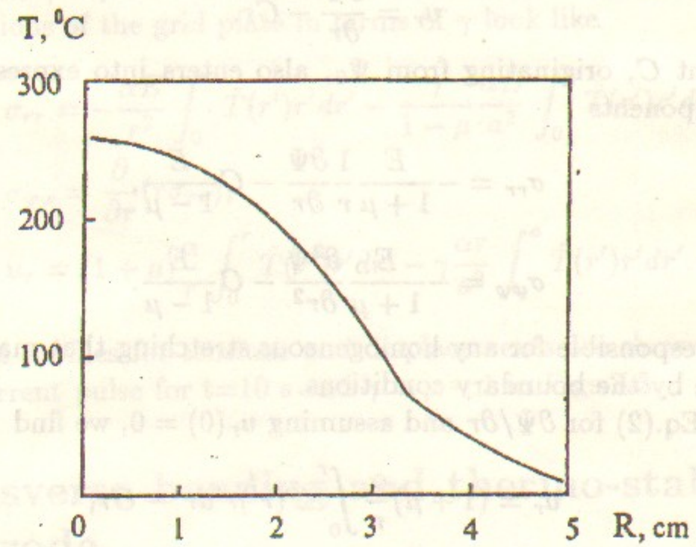

Figure 1: Electrode temperature vs. radius.

2.2 Estimates of thermomechanical tensions

A flat, independent of z ($\sigma_{zz} = \sigma_{zx} = \sigma_{yz} = 0$) deformation of a plate can be described in terms of the thermoelastic potential Ψ, which satisfies the following equation:

$$\Delta\Psi = (1+\mu)\alpha\hat{T}.$$

Here α is the thermal expansion coefficient, $\hat{T} = T - T_i$, where T_i is the initial temperature, and μ is the Poisson coefficient. The 2D vector of dislacements is given in terms of Ψ by the relationship

$$\vec{u} = \nabla(\Psi - \Psi_0),$$

where Ψ_0 describes the effect of boundary conditions and satisfies

$$\frac{\partial^2}{\partial x \partial y}\Psi_0 = 0.$$

In the case when the temperature distribution and the boundary conditions are axisymmetric, the above expressions reduce to

$$\frac{1}{r}\frac{\partial}{\partial r}(r\frac{\partial\Psi}{\partial r}) = \alpha(1+\mu)\hat{T}(r), \tag{2}$$

and

$$u_r = \frac{\partial\Psi}{\partial r} - Cr.$$

The constant C, originating from Ψ_0, also enters into expressions for the tension components

$$\sigma_{rr} = -\frac{E}{1+\mu}\frac{1}{r}\frac{\partial\Psi}{\partial r} - C\frac{E}{1-\mu},$$

$$\sigma_{\varphi\varphi} = -\frac{E}{1+\mu}\frac{\partial^2\Psi}{\partial r^2} - C\frac{E}{1-\mu}.$$

Thus, C is responsible for any homogeneous stretching that may be imposed on the plate by the boundary conditions.

Solving Eq.(2) for $\partial\Psi/\partial r$ and assuming $u_r(0) = 0$, we find

$$u_r = (1+\mu)\frac{\alpha}{r}\int_0^r \hat{T}(r')r'dr' - Cr,$$

$$\sigma_{rr} = -\frac{\alpha E}{r^2}\int_0^r \hat{T}(r')r'dr' - C\frac{E}{1-\mu}, \tag{3}$$

$$\sigma_{\varphi\varphi} = \frac{\partial}{\partial r}(r\sigma_{rr}).$$

As an approximation, let's use the following formulation of the boundary problem: the round grid plate of radius a is fixed in an elastic holder, that is an infinite flat plate of the same thickness as the grid, but with different Young modulus E' and Poisson coefficient μ'. Introducing

$$\beta \equiv \frac{E'}{E}\frac{1+\mu}{1+\mu'}$$

we note that $\beta \to \infty$ corresponds to the fixed-boundary problem, while $\beta = 0$ represents the free-boundary one.

A holder deformation $u_r = \delta/r$ causes radial stress $\sigma_{rr} = -E'\delta/(1+\mu')r^2$, so that the equivalent boundary condition for the grid is

$$\sigma_{rr}(a) = -\beta\frac{E}{1+\mu}\frac{u_r(a)}{a}. \tag{4}$$

Using solution (3) with this boundary condition we find

$$C = \gamma\frac{\alpha}{a^2}\int_0^a \hat{T}(r')r'dr',$$

where $\gamma \equiv (\beta-1)(\beta/(1+\mu) + 1/(1-\mu))^{-1}$; $\gamma = 1+\mu > 0$ for the fixed boundary, while $\gamma = \mu - 1 < 0$ for the free boundary problem. Radial stresses and deformations of the grid plate in terms of γ look like

$$\sigma_{rr} = -\frac{\alpha E}{r^2}\int_0^r \hat{T}(r')r'dr' - \frac{\gamma}{1-\mu}\frac{\alpha E}{a^2}\int_0^a \hat{T}(r')r'dr', \tag{5}$$

$$\sigma_{\varphi\varphi} = \frac{\partial}{\partial r}(r\sigma_{rr}), \tag{6}$$

$$u_r = (1+\mu)\frac{\alpha}{r}\int_0^r \hat{T}(r')r'dr' - \gamma\frac{\alpha r}{a^2}\int_0^a \hat{T}(r')r'dr'.$$

The radial profiles for tensions and displacements are shown at the end of a beam current pulse for t=10 s and $\gamma = \mu - 1$ in Figs.2-3.

3 Transverse bending and thermo-stability of electrode

In the previous Section we assumed that the temperature is homogeneous over the plate thickness. This requires the momentum caused by the temperature

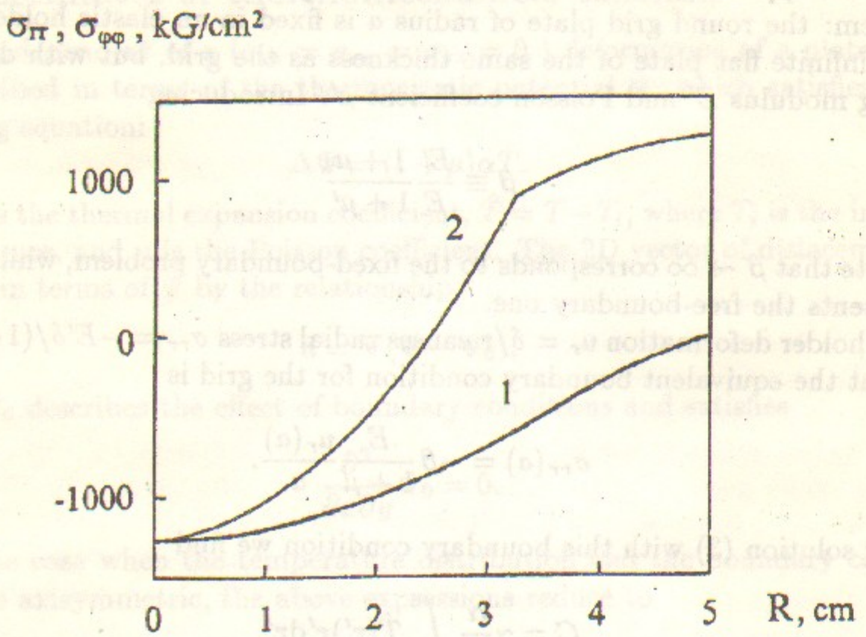

Figure 2: Radial profile of the electrode tensions. 1 - σ_{rr}, 2 - $\sigma_{\phi\phi}$.

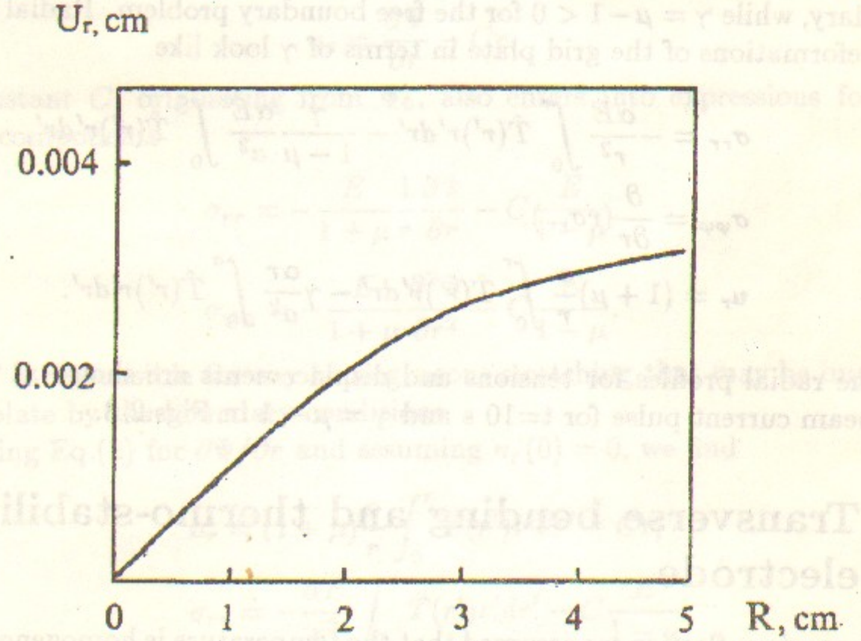

Figure 3: Electrode displacement vs. radius.

inhomogeneity $M_T = \alpha E \int_{-h/2}^{h/2} T(z) z dz \simeq \alpha E \delta T h^2/12$ to be small enough compared to the moment of forces acting in the plane of the electrode:

$$h \frac{1}{r}\frac{\partial}{\partial r}\left(\frac{r^2 \sigma_{rr}}{R}\right) \gg \frac{\alpha E \delta T h^2}{12 a^2}.$$

Here $R = 400$cm is the designed curvature radius. Using expressions for the thermomechanical tensions (5) this condition can be rewritten as

$$\delta T \ll \frac{12 a^2}{Rh}\left(\hat{T} + \frac{2\gamma}{(1-\mu)a^2}\int_0^a \hat{T}(r') r' dr'\right).$$

In our case $a^2/Rh \sim 0.3$, and this condition is well satisfied.

For a heated spherical electrode of radius R one can find its bending (i.e. displacements along the Z axis) using equations (14.4) from [4] and the equation (7.9) from [5](see also [6])

$$D\left\{\nabla^4 \xi^* + \alpha(1+\mu)\nabla^2\left(\frac{dT(x,y,z)}{dz}\right)\right\} = h\frac{1}{r}\frac{\partial}{\partial r}\left(r\sigma_{rr}\frac{\partial \xi}{\partial r}\right), \qquad (7)$$

where $D = \frac{1}{12}Eh^3/(1-\mu^2)$ - is the flextural rigidity of a plate, $\xi(r)$ describes the vertical grid position as

$$\xi = \frac{a^2 - r^2}{2R} + \xi^*,$$

so that ξ^* is the displacement and $\xi^* \ll \xi$ is assumed below the stability threshold; the components of the tension tensor $\sigma_{\alpha\beta}$ are defined in the plate surface by expressions (5),(6).

Let us find solution of equation (7) neglecting tensions caused by an inhomogeneous heating over the plate thickness. Since $\xi^* \ll \xi$, we have

$$h\frac{1}{r}\frac{\partial}{\partial r}\left(r\sigma_{rr}\frac{\partial \xi}{\partial r}\right) \approx -\frac{h}{R}\frac{1}{r}\frac{\partial}{\partial r}(r^2\sigma_{rr}),$$

and, assuming cylindrical symmetry, Eq.(7) takes the form:

$$\left\{\frac{1}{r}\frac{\partial}{\partial r} r \frac{\partial}{\partial r}\right\}^2 \xi^* = -\frac{h}{RD}\frac{1}{r}\frac{\partial}{\partial r}(r^2\sigma_{rr}). \qquad (8)$$

To obtain a simple approximation we shall use the parabolic temperature distribution over the electrode radius $\hat{T} = T_0(1 - r^2/a^2)$. Then,

$\int_0^r \hat{T}(r')r'dr' = \frac{1}{2}T_0 r^2(1 - r^2/2a^2)$, and we get the following expression for the radial tension

$$\sigma_{rr} = \frac{1}{2}\alpha E T_0 \left(\frac{r^2}{a^2} - 2 - \frac{\gamma}{1-\mu}\right).$$

In this approximation equation (8) becomes

$$\left\{\frac{1}{x}\frac{\partial}{\partial x}x\frac{\partial}{\partial x}\right\}^2 \hat{\xi} = \frac{1}{4x}\frac{\partial}{\partial x}(ux^2 - x^4), \tag{9}$$

where $x = r/a$, $u = 2 + \gamma/(1-\mu)$, and $\hat{\xi}$ is the normalized displacement, so that

$$\xi^* = h\frac{\alpha E T_0 a^4}{RD}\hat{\xi}.$$

The general solution of the equation (9) is:

$$\hat{\xi} = -\frac{1}{576}x^6 + \frac{u}{128}x^4 + Ax^2 + Bx^2\ln x + C\ln x + CC.$$

The central boundary conditions $\hat{\xi}, \nabla^2\hat{\xi} < \infty$ at $x = 0$ leads to $B, C = 0$. The constants A and CC are determined by the edge boundary conditions at $x = 1$. For the inflexible edge mounting these conditions are

$$\hat{\xi}, \hat{\xi}'(x) = 0 \quad \text{at} \quad x = 1,$$

and we get the bending amplitude

$$\hat{\xi}(0) = CC = \frac{1}{1152}(9u - 4), \tag{10}$$

or $\xi^* = 0.14$mm in the heating maximum for h=0.2cm and rigidly fixed boundary of the grid.

It follows that the designed curvature can be neglected because it does not change much with heating and its bending height is much less than the electrode thickness

$$\xi_0 = \frac{a^2}{2R} \ll h,$$

while deformations due to the instability will be of the order of a. For the same reason the effects of the nonuniform heating (over the thickness) are also neglected in the following calculations. However, a flat equilibrium state of the electrode with large tensions would become unstable against spontaneous

bending which results in drastic changes of the gaps and misalignments of the beamlets.

To find the lower stability boundary, let us first rewrite Eq.(7) for $\xi = \xi*$ and $\partial T/\partial z = 0$, with assumed cylindrical symmetry:

$$\left\{\frac{1}{r}\frac{\partial}{\partial r}r\frac{\partial}{\partial r}\right\}^2 \xi = -\frac{h}{D}\frac{1}{r}\frac{\partial}{\partial r}\left(r\sigma_{rr}\frac{\partial \xi}{\partial r}\right). \tag{11}$$

For finite bending ξ the radial tension σ_{rr} depends on ξ. However, the linear stability boundary corresponds to such distribution of parameters, when the linearized equation (11) has a non-zero solution, satisfying all boundary conditions. Linearizing Eq.(11) simply means substituting expression (5), found for the flat equilibrim, in place of σ_{rr}.

The order of Eq.(11) can be effectively reduced by integrating it in r and renaming $(\partial\xi/\partial r) = v$:

$$\frac{\partial}{\partial r}\frac{1}{r}\frac{\partial}{\partial r}(rv) - \frac{h}{D}\sigma_{rr}v = 0. \tag{12}$$

The integration constant is set to zero because of requirement $\xi, \nabla^2\xi < \infty$ at $r = 0$. The boundary condition for v at $r = a$ can be taken as $v(a) = 0$ for the fixed edge.

Equation (12) can be solved analytically for the uniform distribution of temperature. In this case it becomes the Bessel equation, indeed, for $\hat{T} = T_0$

$$\sigma_{rr} = -\frac{1}{2}\alpha E T_0(1 + \frac{\gamma}{1-\mu}) = \text{const},$$

and the equation for bending looks like

$$v'' + v'/r + (\kappa^2 - 1/r^2)v = 0, \tag{13}$$

where

$$\kappa^2 = h\sigma_{rr}/D = 6\frac{\alpha T_0}{h^2}(1-\mu^2)(1 + \frac{\gamma}{1-\mu}).$$

The instability threshold can be found as a solution of $J_1(\kappa a) = 0$, or $\kappa^2 a^2 \leq 14.7$ for the fixed edge.

The instability threshold can be also expressed as the limitation on the Young modulus ratio β:

$$\beta \leq \frac{1+\mu}{2Q - 1 + \mu},$$

where $Q = 6\alpha T_0(1-\mu^2)/(h^2 p)$, and $p = 14.7$. Note that for $Q < 0.5(1-\mu)$ there is no limitation on β, meaning that the system is stable even with a rigid holder.

This analysis shows that for $T_0 < 750^oC$ the model system is stable. However, one should have in mind that the above model does not account for nonuniform stresses present in the real system.

4 Summary

From the considerations given in the previous Sections the following conclusions can be drawn.

First, according to numerical simulations, the given heat load to the grids, which are cooled from periphery, causes insignificant changes in the gaps. In fact, their predicted values appear to be small enough so that the beam formation is altered insignificantly. This conclusion was also supported by the testing results. For experimental study of grid deformation a special grid prototype was fabricated. The prototype consists of a vacuum-melted molibdenium grid and a copper holder. Tight thermoconductive joint between the grid and its holder is obtained by rolling an edge of the copper holder to the grid.

The grid prototype was heated by radiation of an ohmically heated tungsten wire. Pulse duration of heating was determined by opening the gating diaphragm installed between the grid and the heater. The heater power was varied up to $1.5kW$. The measured temperature rise at the center of the grid for a heating cycle was 250^oC. The maximum axial displacement of the grid centre was measured to be 75 μm with reasonable reproducibility from pulse to pulse. The observed value of displacement is remarkably smaller in comparison to the theoretical estimate (140 μm) for the grid rigidly fixed at periphery. The observed difference can be attributed to favorable elastic properties of the holder, which apparently allows some edge expansion while inhibiting flexibility. This shows that the proposed design of the grid is characterized by a good quality mounting. However, it may also reflect uncertainties in the definition of the radius of the heated zone a, which can strongly alter the value of the displacement. The amplitude of the displacement is much smaller in comparison with the gap and, therefore, practically does not change characteristics of the ion beam.

Secondly, in accordance with the model prediction, it was observed that the threshold of the dangerous bending instability driven by thermal stresses is not reached.

At the same time, under real conditions of the beam formation, the heat loads may be increased due to higher gas pressures in the gaps and/or non-optimal beam formation. Besides, producing longer beam pulses may become desirable. These problems can be, of course, avoided by increasing the grid thickness. However, this will significantly affect the formation of the elementary beams in the ion-optical system. Since the focusing electric fields inside the deeper beamlets are then diminished, the formation of the beam may deteriorate. This problem was numerically studied in [7], where it is shown that the beam divergence of less than 1^0 can be obtained for the electrode thickness up to 4 mm.

References

[1] E. Hintz and B.Schweer, Plasma Phys. Control. Fusion 37 (1995) A87-A101

[2] G.F Abdrashitov, E.D.Bender, V.I. Davydenko, P.P.Deichuli et al, Proc. 18th Symp. Fusion Techn., Karlsruhe, Germany (1994), p.601

[3] Y. Ohara, M. Akiba, Y. Arakawa, Y. Okumura and J. Sakuraba, J. Appl. Phys. 51, No.7, 3614 (1980)

[4] L.D. Landau, E.M.Lifshic, Theory of elastity, Moscow,Nauka,1987

[5] E.Melan, H.Parcus, Thermal expansions in stationary temperature fields, Wien,1953

[6] B.A.Boley,J.H.Weiner,Theory of thermal stresses,New York,1960

[7] V.I.Davydenko, A.A.Ivanov, A.I. Rogozin and R.Uhlemann, Rev. Sci. Instrum. 68 , No. 3, 1418 (1997)

A. Beklemishev, V. Davydenko, A. Ivanov, and A. Podyminogin

Assessment of thermo-mechanical stresses and stability of ion-source grids with peripheral cooling

Budker INP 97-75

Ответственный за выпуск А.М. Кудрявцев
Работа поступила 25.09. 1997 г.

Сдано в набор 26.09.1997 г.
Подписано в печать 26.09.1997 г.
Формат бумаги 60×90 1/16 Объем 1.3 печ.л., 1.0 уч.-изд.л.
Тираж 100 экз. Бесплатно. Заказ N° 75

Обработано на IBM PC и отпечатано на
ротапринте ГНЦ РФ "ИЯФ им. Г.И. Будкера СО РАН",
Новосибирск, 630090, пр. академика Лаврентьева, 11.